

Magnetoresistance in dotlike and antidotlike structures

G. Berthold, J. Smoliner, V. Rosskopf, E. Gornik, G. Böhm, and G. Weimann

Walter-Schottky-Institut, Technische Universität München, Am Coulombwall, D-8046 Garching, Germany

(Received 17 December 1991)

The magnetotransport in a two-dimensional electron gas in strongly modulated potentials is investigated. For dotlike and antidotlike lateral surface superlattices, a well-defined negative-differential-magnetoresistance behavior is observed followed by a large peak at low magnetic fields. Calculating the electron drift in the modulated potential by taking the external electric fields and the Hall field explicitly into account, two different groups of electrons are obtained, which are in a detailed balance. As only one of these groups contributes to the current flow, the occurrence of the negative differential magnetoresistance in two-dimensional lateral surface superlattices is thus explained. Moreover, the observed maximum in the magnetoresistance is also obtained from this model.

Electrons in low-dimensional systems are a topic of increasing interest in the last few years. In such systems of confined geometry and reduced dimensionality, the transport properties are influenced by various effects, whose occurrence depends on the geometric dimensions of the investigated structures and the position of the Fermi level relative to the confining potential. One of the parameters that can be used to classify a lateral surface superlattice is the ratio $\lambda = E_F / eV_m$, where eV_m denotes the potential modulation and E_F the Fermi energy in the system.

In weak linearly modulated potentials, where the Fermi level is much higher than the potential modulation ($\lambda \gg 1$), Weiss *et al.*^{1,2} and Winkler, Kotthaus, and Ploog³ observed magnetoresistance oscillations being equally spaced as a function of $1/B$. The period of these oscillations is determined by the ratio of the Landau radius and the period the modulated potential. For smaller values of λ , these oscillations start to disappear and a positive low-field magnetoresistance is generated, which is related to the ratio of closed and open electron trajectories.⁴ Similar effects also occur in square superlattice geometries⁵ and hexagonal geometry superlattices generated by latex sphere etching masks.⁶

For $\lambda \approx 1$, two additional sets of low-field magnetoresistance oscillations were observed in linearly modulated potentials.⁷ Due to a locally modulated density of states, electrons are transferred between regions of high and low mobility. This leads to resistance maxima each time the electron concentration is high in low-mobility areas and resistance minima, as electrons are transferred into areas of high mobility.

For $\lambda < 1$, the electron gas is constrained in a zero- or one-dimensional system, depending on the geometry of the modulation. In the case of quantum wires, Thornton⁸ showed that an anomalous magnetoresistance peak occurs at a position that scales with the ratio of the Fermi wave vector and the wire width. He explained this behavior as a consequence of diffusive boundary scattering processes at rough interfaces. A similar peak was also observed in antidot superlattices.^{9,10} Using a classical model of ballistic motion, the observed maximum in the

resistivity ρ_{xx} was explained by a magnetic-field-dependent diffusion constant. Most recently, evidence of commensurate orbits impaled upon small groups of antidots was also found.¹¹

In this paper, we investigate the transport properties of dot- and antidot-type lateral surface superlattices (LSSL's) in a regime, where the Fermi energy is in the same order of magnitude as the potential modulation ($\lambda \geq 1$). In both cases, a large negative differential magnetoresistance (NDR) is observed at low magnetic fields, which is followed by a pronounced maximum. To explain this behavior, we calculate the electron drift in a two-dimensional LSSL, taking the external electric field and the Hall field explicitly into account. A detailed balance between two groups of electrons is obtained from our model, whose ratio depends on the magnetic field. As one group of electrons contributes to the current flow while the other does not, the NDR in a two-dimensional LSSL is explained for the first time. In addition, the low-field magnetoresistance maximum is also described.

The samples consist of an unintentionally *p*-type doped GaAs layer grown on a semi-insulating substrate ($N_A < 10^{14} \text{ cm}^{-3}$), followed by an undoped spacer ($d = 120 \text{ \AA}$) and doped $\text{Al}_x\text{Ga}_{1-x}\text{As}$ ($d = 400 \text{ \AA}$, $N_D = 2 \times 10^{18} \text{ cm}^{-3}$, $x = 32\%$). The additional GaAs cap layer was also highly *n*-type doped ($d = 150 \text{ \AA}$, $N_D = 3 \times 10^{18} \text{ cm}^{-3}$). Bar-shaped mesas ($300 \times 100 \mu\text{m}^2$) were etched into the sample and Ohmic contacts were alloyed using Au-Ge. Photoresistant grid structures with a period of $a = 475 \text{ nm}$ and photoresistant dot arrays ($a = 630 \text{ nm}$) were fabricated on the mesas using uv-laser holography. Developing the photoresistance dots and antidots having a diameter of $d \approx a/2$ were obtained. To induce a modulated electron density, the photoresistance patterns were transferred into the GaAs by wet chemical etching ($[\text{H}_2\text{O}]:[\text{H}_2\text{O}_2]:[\text{NaOH}] = 500:2:1$). The resulting potential modulation of $V_m = 9 \text{ meV}$ for a dotlike ($a = 630 \text{ nm}$) and $V_m = 12 \text{ meV}$ for an antidotlike LSSL ($a = 475 \text{ nm}$) was deduced from etch depth-dependent

electron-density measurements on unstructured test samples. Finally, a Au gate was evaporated. The mobility of the samples is $\mu = 7 \times 10^5 \text{ cm}^2/\text{Vs}$ at $T = 4.2 \text{ K}$. A schematic view of the sample is shown in Fig. 1(a).

To investigate the transport properties of these lateral surface superlattices, magnetoresistance measurements were performed in a configuration where the magnetic field is oriented perpendicular to the two-dimensional electron gas. Figure 2 shows the magnetoresistance curves for an antidotlike superlattice (curve *A1*) and a dotlike superlattice (curves *D1* and *D2* for two different gate voltages). At low magnetic fields ($B < 0.1 \text{ T}$), a clear NDMR is evident in all cases. For the antidotlike LSSL, however, this behavior is more pronounced than for the dotlike LSSL. In addition, a large maximum in the magnetoresistance is observed at $B = 0.43 \text{ T}$ for the antidotlike LSSL (curve *A1*) and at $B = 0.3 \text{ T}$ for the dotlike LSSL (curves *D1* and *D2*). This peak is also observed by other groups on antidot lattices.^{8,9} The NDMR has also been seen by several groups, but was never discussed. The inset of Fig. 2 shows the Shubnikov–de Haas oscillations for the antidotlike LSSL (*A1*) up to $B = 4 \text{ T}$.

To explain these properties quantitatively, we now consider electrical transport in a two-dimensional lateral surface superlattice in terms of a classical Drude model. The classical magnetoresistance is given by the expression $\rho_{xx} = m^*/(Ne^2\tau)$, where m^* denotes the effective mass, e the electron charge, τ the scattering time, and N the number of electrons per unit area that contribute to the current flow. In our model, N is obtained from

$$N(B) = P(B)n_s \int_{E_F - kT}^{E_F + kT} \frac{1}{E_F} - f(E) dE, \quad (1)$$

where n_s is the two-dimensional electron concentration, $f(E)$ the Fermi distribution, and $P(B)$ the magnetic-field-dependent percentage of electrons that contribute to the current flow. Note that such effective electron densities were also used to describe the influence of random inhomogeneities on the magnetotransport properties of bulk crystals.¹²

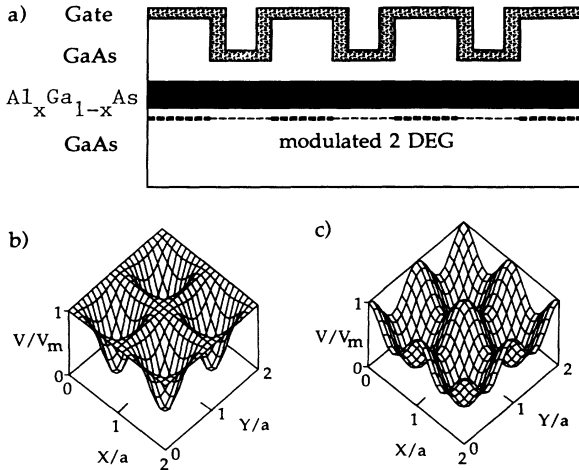


FIG. 1. (a) A cut through the sample. The shapes of the dotlike potential (b) for $\kappa=1$ and the antidotlike potential (c) for $\kappa=0$ are also shown.

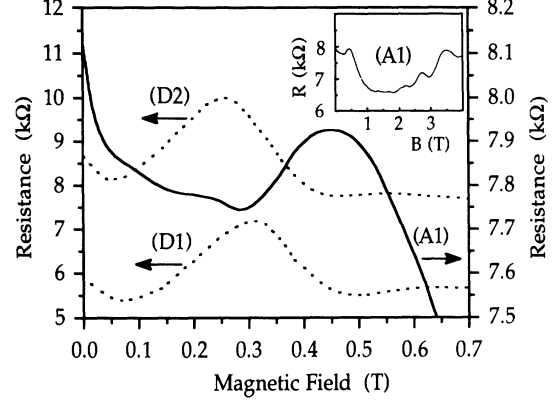


FIG. 2. Measured low-field magnetoresistance of an antidotlike LSSL (curve *A1*) and a dotlike LSSL. Curve *D1* was traced at $V_g = -50 \text{ mV}$, curve *D2* at $V_g = -100 \text{ mV}$. The inset shows the magnetoresistance for larger fields, where Shubnikov–de Haas oscillations are clearly resolved.

To calculate $P(B)$, we now consider the classical Hamiltonian, including the two-dimensional periodic potential $V(x,y)$ and the applied magnetic field perpendicular to the LSSL. In addition to calculations performed by other groups,^{3,8} we also include the external electric field \mathbf{E}_{ext} (x direction) and the Hall field \mathbf{E}_{Hall} (y direction). Using a symmetric gauge $\mathbf{A} = \frac{1}{2}(-By, Bx, 0)$, the Hamiltonian has the following form:

$$H = \frac{(p_x + eBY/2)^2}{2m^*} + \frac{(p_y - eBx/2)^2}{2m^*} + V(x,y) + eE_{\text{ext}}x + eE_{\text{Hall}}y. \quad (2)$$

The Hall field is given by $E_{\text{Hall}} = (eB\tau/m^*)E_{\text{ext}} = \omega_c\tau E_{\text{ext}}$. Neglecting the higher Fourier components, the periodic potential is given by the expression

$$V(x,y) = \frac{V_m}{4} \left[\cos\left(\frac{2\pi}{a}x\right) + \cos\left(\frac{2\pi}{a}y\right) - \kappa \cos\left(\frac{2\pi}{a}x\right) \cos\left(\frac{2\pi}{a}y\right) + 2 + \kappa \right], \quad (3)$$

$\kappa=1$ stands for a dotlike potential and $\kappa=0$ denotes an antidot-type potential [see Figs. 1(b) and 1(c)]. For our calculations, we used a potential modulation of $V_m = 9 \text{ meV}$ for the dotlike ($a = 630 \text{ nm}$) and $V_m = 12 \text{ meV}$ for the antidotlike ($a = 475 \text{ nm}$) LSSL. Different gate voltages are simulated through different Fermi energies.

The Hamiltonian equations of motion, which are deduced from Eq. (2), were solved numerically for a set of 588 arbitrary initial starting points (x,y) and momentum vectors (p_x, p_y) . The corresponding kinetic energy was then obtained by $E_{\text{kin}} = E_f - V(x,y)$. After a scattering time $\tau = 2.6 \times 10^{-11} \text{ s}$, which was obtained from the sample mobility, another set of arbitrary initial conditions simulates the scattering processes in the modulated system. To take the inelastic-scattering processes into account, the new set of initial conditions is always taken at a constant energy, which guarantees that the particles do

not accumulate energy in the average.

The external electric fields ($E_{\text{ext}} \approx 0.3$ V/cm for both samples) are 10^2 – 10^3 times smaller than the internal fields in the LSSL. Therefore, in good approximation, the external electric field will not change the electron energy between two scattering processes. In contrast to that, the situation in momentum space is changed significantly. Two groups of electrons are established, that coexist in a detailed balance. The first group $P(B)$ has a drift in the direction of the external field. Typical trajectories for the antidotlike LSSL are shown in Fig. 3, where the nodes of the grid represent the maxima in the modulated potential. Curve (a) is obtained at $B = 0.3$ T, where the resulting trajectory is rather chaotic, but with a clear drift in the direction of the external field. At $B = 1$ T, curve (b) shows the electron motion in a range where the Hall field is much larger than the external electric field. Thus, a $\mathbf{E}_{\text{Hall}} \times \mathbf{B}$ drift is generated, which is parallel to \mathbf{E}_{ext} . The second group of $[1 - P(B)]$ electrons moves either perpendicular to the external field [curve (c), $B = 0.1$ T] or on closed trajectories [curve (d), 0.5 T]. This kind of orbit always exists as long as the integral $\int (E_{\text{int}} + E_{\text{ext}} + E_{\text{Hall}}) ds$ is zero. Here, the integration is carried out along the trajectory and E_{int} is the internal field resulting from the modulated potential. For closed trajectories this condition can be achieved when the center of the trajectory is not located in the potential minimum between the surrounding antidot curve (d).

To evaluate the number of electrons contributing to the current flow $P(B)$, one has to know how many particles move in field direction [e.g., on trajectories of type (a) and (b)]. For a fixed Fermi level and $B = 0$ T, a significant amount of the electrons channel through the potential valleys perpendicular to the direction of the external field. The other electrons move parallel to the external field E_{ext} or have some random-walk-like behavior with an average drift velocity v_{drift} in the direction of

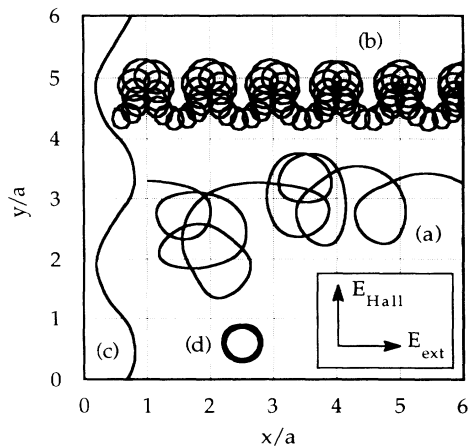


FIG. 3. Typical trajectories in an antidotlike LSSL. Curve (a) ($B = 0.3$ T) and (b) ($B = 1$ T) represent trajectories on which electrons drift in the direction of the external field. Electrons on curve (c) ($B = 0.1$ T) and (d) ($B = 0.5$ T) cannot contribute to the current flow. The nodes of the grid are the maxima of the modulated potential [see also Fig. 1 (c)].

the external field. A look at different potential shapes used in our calculation [Figs. 1(b) and 1(c)] clarifies that the channeling behavior is much more pronounced in the antidotlike LSSL than in the dotlike potential. In the antidotlike LSSL only 50% of the electrons drift in the field direction, whereas 80% drift in the field direction in the dotlike potential. As the electrons that move perpendicular to the external field E_{ext} do not contribute to the current flow, the $B = 0$ T resistance of the nanostructured samples is increased compared to unstructured samples.

We now consider the influence of very low magnetic fields ($B < 0.2$ T) on the electron trajectories. The increasing magnetic field decreases the number of electrons $[1 - P(B)]$ that move perpendicular to the external electric field and increases the relative number of electrons $P(B)$ (Fig. 4). The motion of these electrons can be described as a random walk with an average velocity v_{drift} in the direction of E_{ext} . This behavior reflects the fact that in a two-dimensional cosine-shaped potential, no closed orbits can exist at very low magnetic fields, and the normally expected $\mathbf{E} \times \mathbf{B}$ drift is suppressed. The increased number of electrons, that are drifting in the direction of the external field results in a NDMR. Such a behavior turns out to be characteristic for all two-dimensional periodic potentials and is independent of the ratio of Fermi energy and potential modulation.

If B increases further ($B > 0.2$ T), the interplay between the Hall field $E_{\text{Hall}} = \omega\tau E_{\text{ext}}$ and the Lorentz force $e\mathbf{v} \times \mathbf{B}$ strongly influences the trajectories in the two-dimensional modulated potential. In this regime, the Lorentz force induces an increasing number of closed orbits. Simultaneously, $P(B)$ is reduced due to a decreasing number of electrons drifting in the direction of the external field.

At even higher magnetic fields ($B > 0.25$ and 0.5 T for the dotlike and antidotlike LSSL, respectively), where the diameter of the cyclotron orbit matches the period of the

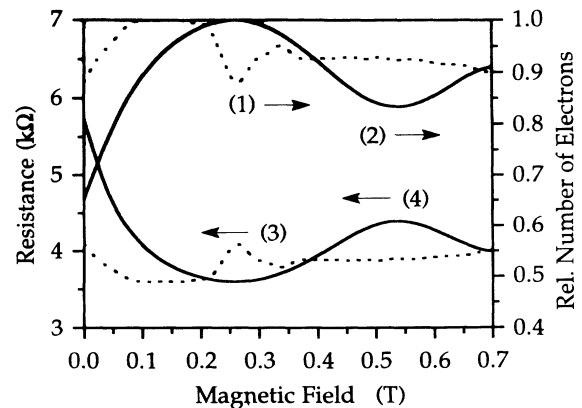


FIG. 4. Calculated magnetoresistance for the antidotlike [solid curve (4)] and the dotlike LSSL [dotted curve (3)] for $V_g = -50$ mV. The negative magnetoresistance is more pronounced in the case of the antidot LSSL than in the dotlike LSSL. The calculated relative number of electrons $P(B)$ that participate in the current for the antidotlike [solid curve (2)] and the dotlike LSSL [dotted curve (1)] is shown on the right scale.

LSSL, the Hall field E_{Hall} is so large that the stability of the closed trajectories is destroyed and a regular $E_{\text{Hall}} \times \mathbf{B}$ drift behavior comes up. This means that more and more carriers drift in the direction of the external field, and $P(B)$ increases. The interplay between the Hall field and the Lorentz force leads to a minimum in $P(B)$. Therefore, a maximum in the magnetoresistance is expected in the range where the diameter of the cyclotron orbit matches the period of the LSSL.

We now compare the theory with experimental results. As a consequence of our model, the enhancement in the resistance at $B = 0$ T is due to a lowered amount of electrons participating to the current flow and not due to a decreased value of the scattering time τ . This is verified by the fact that the calculated sample resistance at $B = 0$ T fits well to the experimental data if the scattering time τ of the unstructured samples is used. From the experimental data (Fig. 2) and the calculated results (Fig. 4) it is obvious that the NDMR at very low magnetic fields is more pronounced for an antidotlike potential than for a dotlike potential. This behavior is explained by the fact that the antidotlike LSSL enables the electrons to channel through the potential valleys perpendicular to the direction of the external field. In a dotlike potential such channels do not exist, resulting in a less-pronounced NDMR behavior that is predicted by our theory.

From the measured and calculated results, we find that the magnetoresistance peak positions B_p agree quite well. For the antidotlike potential, which has a period 475 nm, we obtain a value $B_p^{\text{calc}} = 0.51$ T and an experimental value of $B_p^{\text{expt}} = 0.43$ T. For the dotlike potential ($a = 630$ nm) we also find that the gate-voltage dependence of the peak positions is predicted correctly by our model. At more negative gate voltages, the peak is shifted to lower magnetic fields. For $V_g = -50$ mV, we obtain a peak position of $B_p^{\text{calc}} = 0.26$ T, which is shifted to $B_p^{\text{calc}} = 0.22$ T at $V_g = -100$ mV. Experimentally these peaks are observed at $B_p^{\text{expt}} = 0.30$ T (*D1*) and $B_p^{\text{expt}} = 0.25$ T (*D2*), respectively. As no fitting parameters were used, the quantitative value of the calculated mag-

netoresistance is in reasonably good agreement with the experimental data. For the magnetoresistance of the antidot sample (curve *A1* in Fig. 2), we also find a second very small peak at approximately $B = 0.2$ T, which is not understood yet. The remaining deviations between the experiment and our theory, e.g., the small shift in the position of the peaks and the different shape of the magnetoresistance, might be removed if a self-consistent potential and a spatial dependence of the scattering time in the etched and nonetched areas are taken into account. Note that the beginning of Landau quantization at about $B = 0.6$ T limits our semiclassical description of the situation.

According to the literature,⁹ samples having a low mobility ($\mu < 25\,000$ cm²/V s) do not exhibit a magnetoresistance peak at low magnetic fields. In these samples, the scattering time is too short to enable closed orbits. Thus a magnetoresistance peak cannot occur according to our model. However, trajectories perpendicular to the electric-field direction still exist, which explains the well-defined NDMR in such samples.⁹

In summary, we have investigated the transport properties of dotlike and antidotlike LSSL's in the presence of a low magnetic field. In both types of samples, a well-defined NDMR followed by a large resistance maximum is observed. Taking explicitly the external electric field and the Hall field into account, we find that the modulated potential induces trajectories on which electrons move perpendicular to the direction of the external field. For a limited range of magnetic fields, closed orbits can also exist in the superlattice potential. By calculating the number of electrons in these orbits, the NDMR and the large maximum in the magnetoresistance are quantitatively explained.

The authors are grateful to J. A. Brum and W. Demmerle for helpful discussions. This work was sponsored by Deutsche Forschungsgemeinschaft, Project No. Go469/4-1.

¹D. Weiss, K. v. Klitzing, K. Ploog, and G. Weimann, Europhys. Lett. **8**, 179 (1989).

²D. Weiss, K. v. Klitzing, K. Ploog, and G. Weimann, Surf. Sci. **229**, 88 (1990).

³R. W. Winkler, J. P. Kotthaus, and K. Ploog, Phys. Rev. Lett. **62**, 1177 (1989).

⁴P. H. Beton, E. S. Alves, P. C. Main, L. Eaves, M. W. Dellow, M. Henini, O. H. Hughes, S. P. Beaumont, and C. D. W. Wilkinson, Phys. Rev. B **42**, 9229 (1990).

⁵E. S. Alves, P. H. Beton, M. Henini, L. Eaves, P. Main, O. H. Hughes, G. A. Toombs, S. P. Beaumont, and C. C. W. Wilkinson, J. Phys. C **1**, 8257 (1989).

⁶H. Fang and P. J. Stiles, Phys. Rev. B **41**, 10 171 (1990).

⁷G. Berthold, J. Smoliner, W. Demmerle, F. Hirler E. Gornik, G. Böhm, and G. Weimann, Semicond. Sci. Technol. **6**, 709 (1991).

⁸T. J. Thornton, M. L. Roukes, A. Scherer, and B. P. van de Gaag, Phys. Rev. Lett. **63**, 2128 (1989).

⁹A. Lorke, J. P. Kotthaus, and K. Ploog, Phys. Rev. B **44**, 3447 (1991).

¹⁰K. Ensslin and P. M. Petroff, Phys. Rev. B **41**, 12 307 (1990).

¹¹D. Weiss, M. L. Roukes, A. Menschig, P. Grambow, K. v. Klitzing, and G. Weimann, Phys. Rev. Lett. **66**, 2790 (1991).

¹²C. Herring, J. Appl. Phys. **31**, 1939 (1960).